ELSEVIER

Cement & Concrete Composites 22 (2000) 175–185

Cement & Concrete Composites

Effect of fly ash on concrete reinforcement corrosion studied by EIS

M.F. Montemor [a,*], A.M.P. Simões [a], M.M. Salta [b]

[a] *Instituto Superior Técnico, Chemical Engineering Department, Av. Rovisco Pais, 1049-001 Lisboa, Portugal*
[b] *Laboratório Nacional de Engenharia Civil, Av. Brasil, 1700-066 Lisboa, Portugal*

Received 3 March 1999; accepted 11 January 2000

Abstract

The corrosion process of steel embedded in concrete with various amounts of fly ash (up to 50% of the total binder) was tested under complete and partial immersion, in sodium chloride solution. The corrosion process was followed by monitoring of open circuit potential (OCP) and electrochemical impedance spectroscopy (EIS). Fly ash addition has led to a raise of concrete resistivity and of the time for corrosion initiation and to a decrease of corrosion rate.

Keywords: Corrosion; Reinforcement; Fly ash; Impedance; EIS; Electrochemical techniques

1. Introduction

Steel embedded in concrete is protected against corrosion by both a chemical and a physical mechanism. Chemical protection is provided by the high pH (12.5–13.5) of the concrete interstitial solution, which causes passivation of the reinforcing steel. Concrete also provides physical protection, by hindering the access of aggressive agents. Severe corrosion problems, however, occur in many structures. Most frequently, corrosion is induced by the ingress of chloride ions (Cl^-), which leads to a local destruction of the passive film [1].

Addition of fly ash to concrete has become common practice in recent years. Fly ash is a finely divided residue resulting from powdered coal combustion and acts as a pozzolanic material [2], i.e., the particles react with water and lime to produce cementitious products [2,3]. Reasons for fly ash addition include economy and enhancement of certain properties of fresh concrete [3] (workability and pumpability) and of hardened concrete [3,4]. Studies have been published concerning the effect of fly ash on concrete porosity and resistivity [5], pore solution chemistry [2,6], oxygen and chloride ion diffusivity [5–9], carbonation rates [10,11] and passivation [12]. Nevertheless, attention should be focused on the role of fly ash in the corrosion mechanism, especially on what concerns chloride-induced corrosion.

The corrosion process of steel in concrete can be followed using several electrochemical techniques. Monitoring of open circuit potential (OCP) is the most typical procedure to the routine inspection of reinforced concrete structures [13–15]. Its use and interpretation are described in the ASTM *Standard Test Method for Half-Cell Potential of Reinforcing Steel in Concrete*. Potential readings, however, are not sufficient as criterion, since they are affected by a number of factors, which include polarisation by limited diffusion of oxygen [16,17], concrete porosity [18] and the presence of highly resistive layers [18].

Measurement of d.c. polarisation resistance with ohmic drop compensation has been applied since the 1970s and provides information about the corrosion rate [19–24]. In the literature some criteria relating the corrosion rate obtained from d.c. polarisation measurements and the probability of corrosion and/or expectable lifetime were published [25–27]. According to Moosavi et al. [25] the following criteria can be applied:

Corrosion rate (μm/yr)	Degree of corrosion
<0.01	Insignificant (passive)
<1.0	Low
1–10	Moderate
10–30	High
>30	Very high

* Corresponding author. Fax: +351-218404589.
E-mail address: pcfatima@alfa.ist.utl.pt (M.F. Montemor).

0958-9465/00/$ - see front matter
PII: S0958-9465(00)00003-2

In recent years non-d.c. techniques, namely a.c. impedance [28–38] and galvanostatic pulse [16,32–35] have been used to characterise the corrosion process of steel in concrete. Among the advantages of a.c. impedance are the use of very small signals that only minimally disturb the electrode properties to be measured, and the possibility of corrosion rate determination in low conductivity media, where d.c. techniques are affected by a number of errors. However, interpretation of impedance spectra is sometimes difficult, especially in the presence of localized corrosion. Various approaches have been proposed for improving the applicability of a.c. techniques in the study of pitting [39–41].

In this work, laboratory tests were performed on concrete samples with different amounts of fly ash, exposed to chloride environments. OCP and Impedance spectroscopy were applied in order to study the corrosion process induced by chloride ion and the effect of fly ash.

2. Experimental

2.1. Concrete and fly ash

Ordinary portland cement and type-C fly ash were used in concrete preparation (Table 1). The mixing proportions were the following: portland cement plus fly ash: 350 kg; water: 200 l; sand: 1400 kg; aggregates: 360 kg. Fly ash was added in partial substitution of portland cement in the proportions of: 50, 30 and 15 (wt%). Samples with no fly ash were also prepared. The water/binder ratio was in all cases 0.57.

Two commercial steel rebars (type A-10) with a diameter of 1 cm, previously polished with a 600 silicon carbide (SiC) grit emery paper, were embedded in each concrete block, with a concrete cover of 1 cm (Fig. 1).

Table 1
Chemical analysis of the Portland cement and the fly ash used in the concrete (wt%)

	Cement	Fly ash
Insoluble residue	1.10	
Ignition loss	3.88	3.27
SiO_2	19.23	53.62
Al_2O_3	6.89	28.15
CaO	60.69	1.97
MgO	3.15	1.06
SO_3	1.67	0.32
Na_2O	0.52	0.52
K_2O	0.74	2.51
Cl^-	<0.02	0.004
TiO_2	–	1.40
Fe_2O_3	–	6.64
P_2O_5	–	0.17

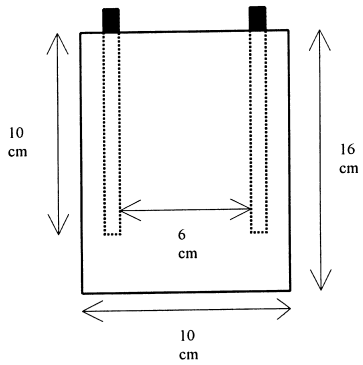

Fig. 1. Scheme of the concrete blocks. Cover thickness = 1 cm; steel bar diameter = 1 cm.

With this geometry, the distance between the inner surface of the steel rebars was 6 cm and the embedded area of each electrode was 32.2 cm^2.

Concrete blocks were cured during 1 week in a saturated humidity chamber before immersion in the aggressive solutions.

2.2. Exposure

Reinforced concrete blocks were either vertically immersed to a depth of 6 cm (partial immersion) or fully immersed in a 3 wt% NaCl solution in distilled water. Under these conditions only chloride-induced corrosion occurred, since the high content of water impeded carbonation of the concrete [1]. Electrochemical tests were made during immersion, and blocks were broken at the end of the tests, for visual inspection. A minimum of two blocks for each condition was tested.

2.3. Electrochemical techniques

The OCP of each steel bar was measured vs. the saturated calomel electrode (SCE). A sponge soaked with the NaCl solution was placed between the tip of the reference electrode and the surface of the concrete, to provide ionic conduction. The measurements were made at sites on the surface located as close as possible to the rebars, using a high impedance voltmeter (10 MΩ). Since the potential measurements were made across a concrete cover thickness of only 1 cm and the concrete was permanently wet, no correction of the measured potentials was made.

Electrochemical impedance spectroscopy (EIS) measurements were made with a two-electrode system, between the identical steel bars of each concrete block, as used by Dawson et al. [28]. Measurements were made using a 1255 Solartron FRA (50 kHz down to 1 mHz) and a 1286 Solartron Electrochemical Interface. A 10 mV (r.m.s.) sine wave was applied. All the experiments were performed using the same arrangement in order to

minimize errors induced by the geometry and thus to allow the comparison of results. Numerical fitting of the impedance data was made using specific software.

3. Results

3.1. Complete immersion

The potential evolution for the steel embedded in concrete of various compositions is presented in Fig. 2. In spite of the dispersion in the readings, some trends can be observed. Thus, during the first days of immersion (1–2 weeks), the readings were in the range −250 to −150 mV, corresponding to a state of passivity, according to the *Pourbaix* diagram [42]. After that period, a slow potential decay towards more negative values was observed. After 1 month of immersion, large fluctuations between −800 and −400 mV were found, until after about 5–6 months more stable potential readings were registered. Those readings were close to −600 mV. They seemed to be independent of the fly ash content and correspond to a steady-state condition.

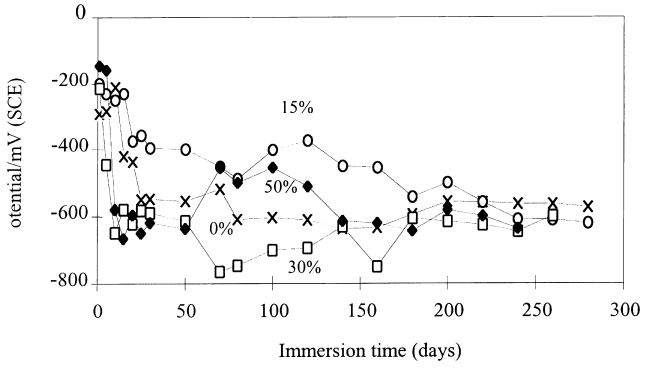

Fig. 2. OCP evolution of concrete samples immersed in a 3% NaCl solution.

Fig. 3 shows typical impedance spectra obtained on the samples with different fly ash content after 1 week of immersion in 3% NaCl solution. Above 100 rad/s the electric resistivity of concrete is measured. At this stage it was practically independent of the composition, except for the sample with 50% of fly ash. At lower frequencies a capacitive behaviour is observed, characterised by a slope of −1 in the Bode magnitude plot. Due to a large scatter in the readings the spectra could not go to very low frequencies, particularly in the sample with 50% of fly ash.

The spectra can be described by an electric resistance in series with a RC network (Fig. 4). The series resistance (R_s) accounts for the ionic conduction in the electrolyte filling the pores, whereas the other elements refer to the double layer capacitance at the steel/concrete interface (C_{dl}) and the charge transfer resistance (R_{ct}). Curve d in Fig. 3 was fitted using this RC network. The charge transfer resistance is very high (>10^6 Ω cm^2) and could not be measured in the range of frequencies tested. The electric resistance and the capacitance were ≈10^3 Ω cm^2 and ≈20 μF/cm^2, respectively.

After 180 days the shape of the spectra was essentially the same, but with a significant rise in the concrete resistance, particularly for the higher fly ash contents (Fig. 5). Concomitantly, a change in the slope of the magnitude spectra to approximately −0.7 was observed, revealing a deviation from the capacitive behaviour. Finally, at the other end of the spectra, above 10^4 rad/s, one other relaxation process was observed in many of

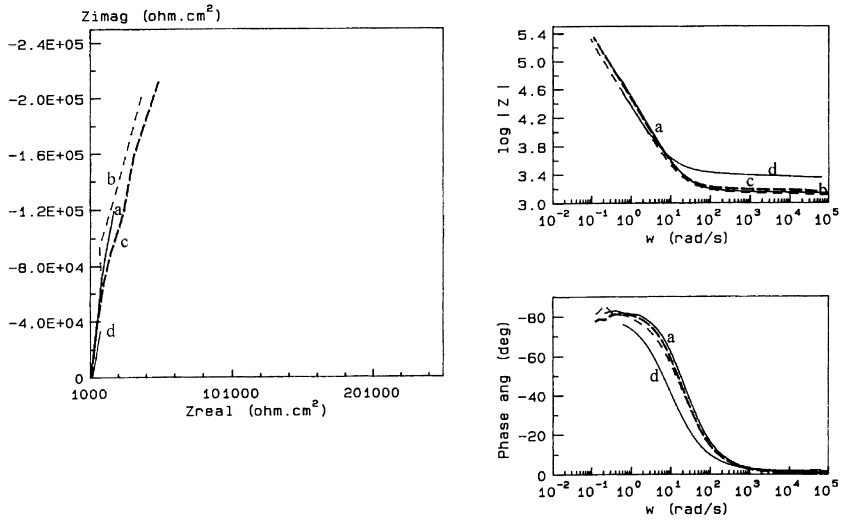

Fig. 3. Impedance spectra of concrete samples after 7 days of immersion in 3% NaCl: without fly ash (a) and with various fly ash contents: 15% (b); 30 % (c); 50% (d).

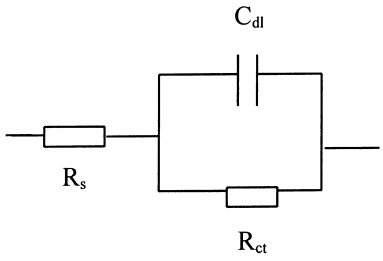

Fig. 4. Equivalent circuit for passive steel in concrete.

the samples, being more evident in the concrete with 50% of fly ash (curve d in Fig. 5). This process was characterised by capacitances of a few nF/cm^2.

The impedance data can help the interpretation of the potential readings. For passive steel immersed in chloride solution, a potential drop usually reveals a transition from passivity to activity, and thus of high corrosion rates. The impedance measurements, however, have revealed large values for charge transfer resistance (above 10^6 Ω cm^2), whereas the values for the OCP were more negative than those expected in a situation of active iron dissolution. This is explained by the limited access of oxygen in the concrete, which leads to concentration polarisation of the cathodic reaction. Under these conditions corrosion occurred at low rate, as confirmed by the existence of small pits on the rebars at the end of the test.

The values of concrete resistance obtained from impedance measurements can be converted into resistivity values, after taking account of the concrete thickness across which measurements were made. For the samples fully immersed in the NaCl solution, the resistivity (ρ) raised more significantly during the first 2–3 months of immersion (Fig. 6), and at a slower rate after this period, as the hydration and pozzolanic reactions approached equilibrium. The evolution of resistivity was different for the various compositions tested. Thus, for the samples with no fly ash, it increased by a factor of 4, whereas for the samples with 50% of fly ash addition, the factor was nearly 40. Thus, although at the end of the curing in the humidity chamber the different types of concrete revealed an identical resistivity, those with fly ash reached significantly higher values of ρ after the completion of the hydration processes. The evolution depicted in Fig. 6 agrees with the known fact that the presence of fly ash is responsible for enhanced concrete resistivity, although longer curing times are needed to achieve it. Therefore, the raise in resistivity after the cure in the chamber was more significant in the samples with higher fly ash content, whereas in the sample with no fly ash most of the cure must have taken place inside the chamber, before exposure. The values are in the same range as some determined by other authors [28,43] and approximately correspond to an exponential law, as previously reported [44,45].

In a different test, concrete blocks without fly ash were immersed in 3% NaCl solution, during 330 days, then dried in air during 90 days and at last partially re-immersed in 3% NaCl. During the first immersion period the potential readings (Fig. 7) were very similar to those observed in Fig. 2, with stable values below −600 mV after about 150 days. During air exposure a rise to less negative values, in the range −400 to −500 mV was detected, whereas after re-immersion a small decay was observed again. Visual inspection of rebars showed severe attack on nearly one third of the exposed area. Fig. 8 depicts the impedance spectra obtained from these

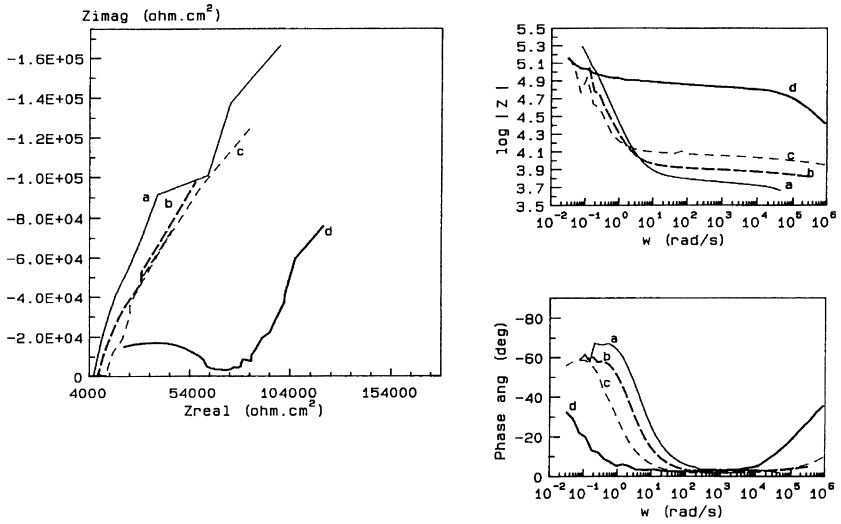

Fig. 5. Impedance spectra of concrete samples after 180 days of immersion in 3% NaCl: without fly ash (a) and with various fly ash contents: 15% (b); 30 % (c); 50% (d).

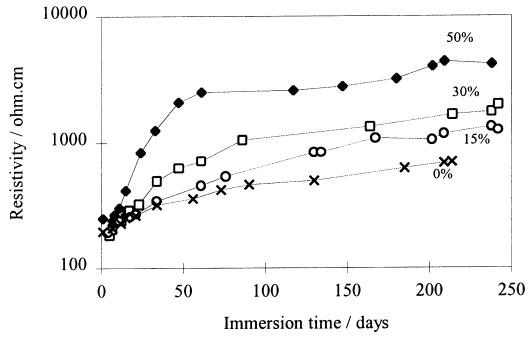

Fig. 6. Evolution of resistivity of samples fully immersed in a 3% NaCl solution.

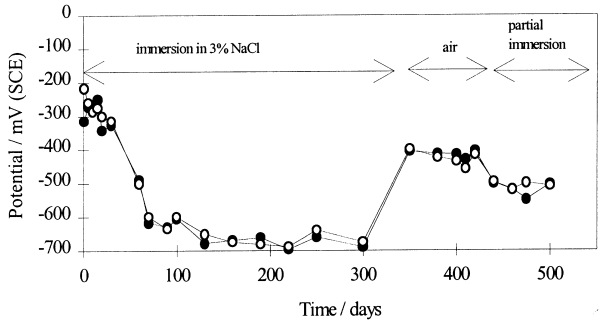

Fig. 7. OCP evolution of concrete samples (without fly ash) submitted to different exposure conditions.

blocks, together with their numerical fittings. Curve a was fitted using the equivalent circuit depicted in Fig. 4, whereas for curves b, c and d the equivalent circuit in Fig. 9 was used. This circuit includes the series resistance (R_s), above discussed, the double layer capacitance (C_{dl}) and the charge transfer resistance (R_{ct}), which accounts for the dissolution processes at the steel/concrete interface, a Warburg impedance (W) describing the transport of charged species and finally a parallel circuit (R_{HF}, C_{HF}) accounting for the high frequency relaxation process. This high frequency process, observed in many spectra, had a capacitance C_{HF} in the range 1–100 nF/cm^2, and a resistance that increased with time and with the amount of fly ash.

This equivalent circuit gives a very general description of the steel/concrete system, and usually only some of the elements are observed in a spectrum. For example, in Fig. 8, the Warburg impedance is detected only in curve d. A similar circuit was used by Dawson et al. [28] for chloride-induced corrosion of steel in concrete.

Large changes in the spectra have occurred both with time and with the different exposure conditions – Fig. 8. At the beginning of immersion, as stated above, the capacitive behaviour of the spectra revealed steel passivity, with a slope of approximately −1 (curve a). In this situation the charge transfer resistance was very high (>10^6 Ω cm^2). After approximately 240 days (curve b) of full immersion, the charge transfer resistance decreased to approximately 3×10^5 Ω cm^2, whereas a slope of −0.7 in the Bode plot revealed deviation from a purely capacitive behaviour. At the same time the potential readings were below −550 mV, revealing active corrosion controlled by the diffusion of oxygen. After removal from the solution, the charge transfer resistance became smaller ($\approx1\times10^5$ Ω cm^2), leading to a decrease in the slope of the spectrum to values around −0.5 (curve c) and consequently to a decrease in the phase angle. This situation, in which high corrosion rates were expected due to the facilitated access of oxygen from the atmosphere, was characterised by potential values in the range −400 to −500 mV. After partial immersion of the sample (curve d), a large decrease was observed both in the slope (≈ -0.3) and in the charge transfer resistance ($\approx1\times10^4$ Ω cm^2). Under these conditions, a Warburg impedance developed at very low frequencies, revealing a rapid corrosion process occurring under mass transfer control. The slope of log|Z| and the charge transfer resistance obtained from numerical fitting of the data are presented in Table 2 and Fig. 10. From that data, the following approximate correlation was found between the charge transfer resistance (R_{ct}) and the slope of the Bode plot:

Slope ≈ −1 to −0.8	$R_{ct} > 10^6$ Ω cm^2
Slope ≈ −0.8 to −0.6	$10^6 < R_{ct} < 10^5$ Ω cm^2
Slope < −0.6	$R_{ct} < 10^5$ Ω cm^2

The slope of the |Z| plot thus seems to reflect the variations of the charge transfer resistance. This relation, however, is affected by a number of factors, namely the resistance of the concrete interstitial solution. In order to account for those effects some numerical modelling was performed (Fig. 11). In those simulations, the charge transfer resistance was kept constant, with a value of 1×10^5 Ω cm^2, a value that seems to correspond to the edge between the situations of concentration polarisation and pitting corrosion. According the results obtained in this work, the value of R_s is generally 10–20 times lower than R_{ct}. The curves depicted in Fig. 11 were obtained using the ratio R_{ct}/R_s as 20, 10, 5 and 2.5. As expected, when the R_{ct}/R_s ratio is small, the slope decreases. However, for the first three curves, the effect is not very significant. The effect of R_s on the slope is more evident for lower R_{ct}/R_s ratios, especially for the lowest ratio ($R_{ct} = 1\times10^5$ and $R_s = 4\times10^4$ Ω cm^2). Results obtained in this work always revealed R_{ct}/R_s ratios above 4. The smaller experimental ratios were observed for curves c and d in Fig. 8(B), corresponding to ≈5 and ≈4, respectively. Thus, it seems that the slopes of the experimental Bode plots obtained in this work are not significantly affected by R_s. Furthermore, according the

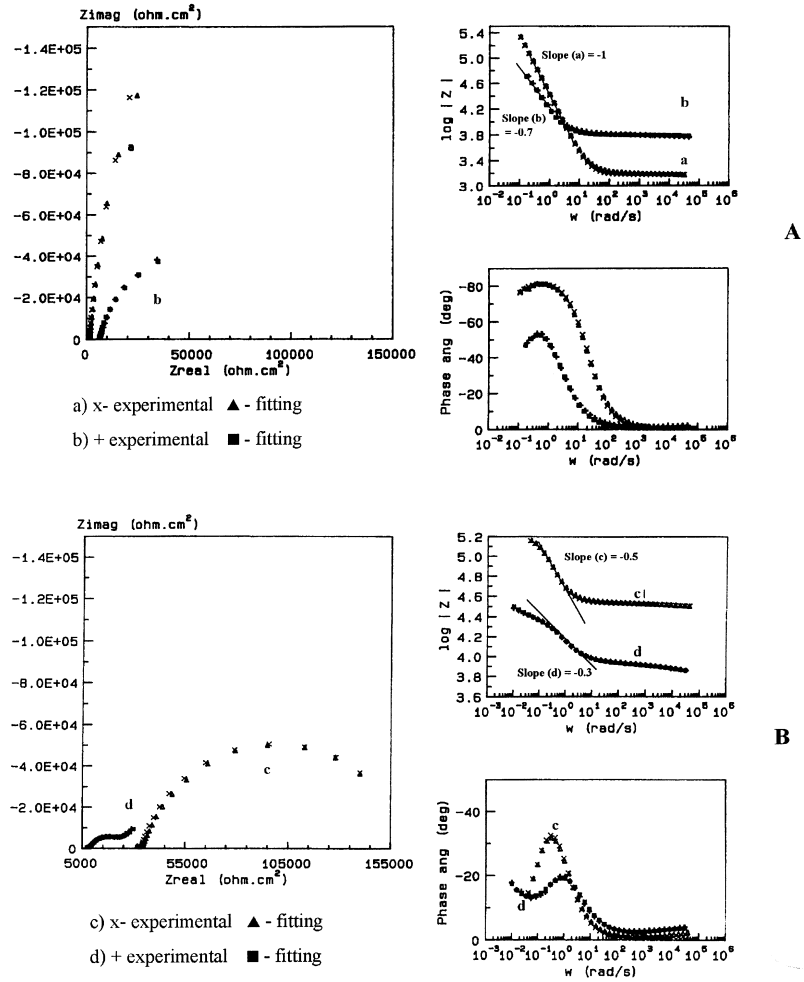

Fig. 8. Impedance spectra obtained for a sample immersed during 330 days in a 3% NaCl solution, then dried at air and immersed in 3% NaCl. (a) 10 days – immersion; (b) 240 days – immersion; (c) 390 days – air; (d) 426 days – re-immersion. Fitting parameters: (a) $R_s = 1.5 \times 10^3\ \Omega\ cm^2$; $R_{HF} = 0\ \Omega\ cm^2$; $C_{HF} = 0\ nF/cm^2$; $R_{ct} > 10^6\ \Omega\ cm^2$; $C_{dl} = 45\ \mu F/cm^2$; $\beta = 5°$. (b) $R_s = 7 \times 10^3\ \Omega\ cm^2$; $R_{HF} = 3.7 \times 10^3\ \Omega\ cm^2$; $C_{HF} = 2.5\ nF/cm^2$; $R_{ct} = 3 \times 10^5\ \Omega\ cm^2$; $C_{dl} = 75\ \mu F/cm^2$; $\beta = 17°$. (c) $R_s = 3 \times 10^4\ \Omega\ cm^2$; $R_{HF} = 5 \times 10^3\ \Omega\ cm^2$; $C_{HF} = 2.5\ nF/cm^2$; $R_{ct} = 14 \times 10^5\ \Omega\ cm^2$; $C_{dl} = 60\ \mu F/cm^2$; $\beta = 14°$. (d) $R_s = 5 \times 10^3\ \Omega\ cm^2$; $R_{HF} = 3 \times 10^3\ \Omega\ cm^2$; $C_{HF} = 5\ nF/cm^2$; $R_{ct} = 2 \times 10^5\ \Omega\ cm^2$; $C_{dl} = 125\ \mu F/cm^2$; $\beta = 25°$.

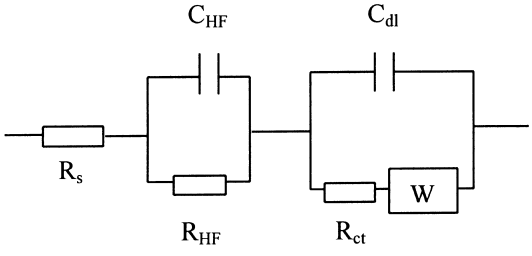

Fig. 9. Equivalent circuit for pitting corrosion of steel in concrete.

experimental results the R_{ct}/R_s ratio is greater than 10 in a situation of passivity, between 5 and 10 when the steel surface reveals weak activity and around 4 under intense localised attack. Similar ratios were also observed in other works [34,46,47] for concrete samples tested under chloride containing environments.

3.2. Partial immersion

The potential evolution was comparable to what was observed in full immersion, although after potential decay the values were less negative then in the absence of oxygen. The potential readings (Fig. 12) were characterised by a passive (>−250 mV) and an active range, $-550 < E < -250$ mV. The passive-to-active transition occurred after about 60 days of immersion for the samples with 0% and 15% of fly ash. For those with 30% of fly ash this transition occurred later, after approximately 480 days. Higher fly ash contents were not used in this set of tests. This behaviour is different from the full immersion, where the time for potential decay seemed to be independent of composition. The justification lies on the fact that, in the presence of oxygen, the potential drop corresponds in reality to pitting initia-

Table 2
Evolution of OCP, charge transfer resistance and slope of the Bode spectra for a sample immersed in 3% NaCl, dried in air and partially re-immersed[a]

Time (days)	Exposure conditions	E (mV) (SCE)	R_{ct} (Ω cm^2)	Slope
7	Immersion	−200	>1.10^6	−1
240	Immersion	−689	3.10^5	−0.7
390	Air	−424	1.10^5	−0.5
426	Re-immersion	−500	2.10^4	−0.3

[a] Values of R_{ct} were obtained from numerical fitting.

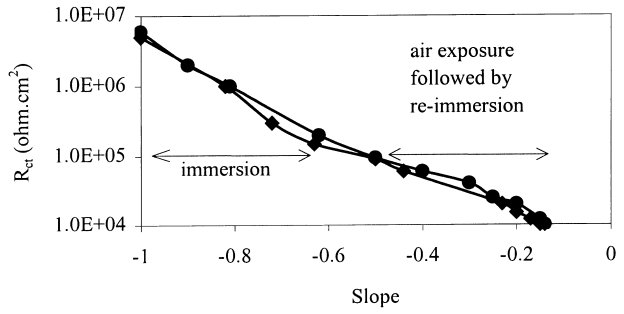

Fig. 10. Charge transfer resistance vs. the slope of the log|Z| Bode plot.

tion, and not to other effects related with instability of the oxide film or oxygen diffusion polarisation, as observed under full immersion.

After 7 days of immersion, the impedance spectra – Fig. 13 – were similar to those observed on the fully immersed samples, with the concrete resistance independent of the composition and in series with the double layer capacitance. After 180 days a splitting of the resistive part of the spectrum was observed – Fig. 14 – whereas at the low frequencies the presence of a corrosion process was observed in the samples with 0% and 15% of fly ash. Fig. 15 depicts the spectra after 540 days, where the state of activity is confirmed for all the samples. The charge transfer resistance and the OCP at various immersion times are presented in Table 3. An increase in the charge transfer resistance with the fly ash content was observed, although this resistance could not be measured in the samples with passive potentials. For 30% of fly ash that increase was by a factor of 4–5.

Concrete resistivity had an evolution comparable to what was observed under full immersion, but with higher values (Fig. 16). This may be due to a lower content of solution in the pores, especially in the parts of the block that were more distant from the solution. Again a decrease in the slope of the Bode plot was observed after the onset of corrosion. By plotting the charge transfer resistance vs. that slope – Fig. 17 – a trend similar to the one observed for total immersion was obtained.

4. Discussion

For the environments studied in this work (full and partial immersion in chloride-containing solutions) and assuming no changes in the pH of the concrete during chloride attack, the potential measurements revealed three different ranges of values. The first one

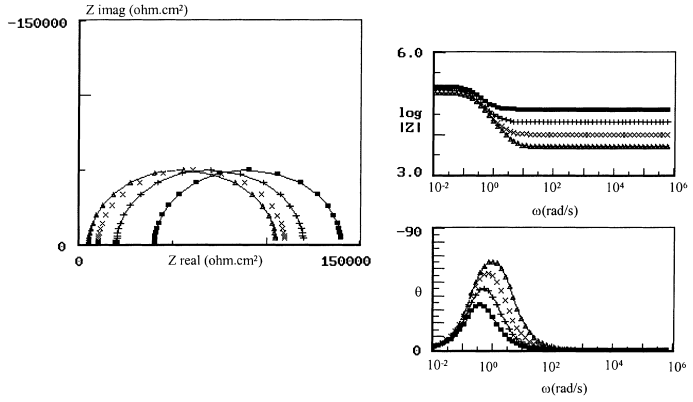

Fig. 11. Theoretical simulation of impedance data: $R_{ct} = 1.10^5$ Ω cm^2; $C_{dl} = 50$ μF/cm^2. ($\triangle$) $R_s = 5.10^3$ Ω cm^2; ($\times$) $R_s = 1.10^4$ Ω cm^2; (+) $R_s = 2.10^4$ Ω cm^2; (■) $R_s = 4.10^4$ Ω cm^2.

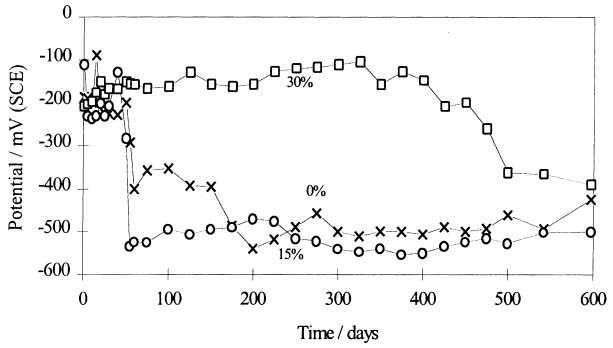

Fig. 12. OCP evolution of concrete samples partially immersed in a 3% NaCl solution.

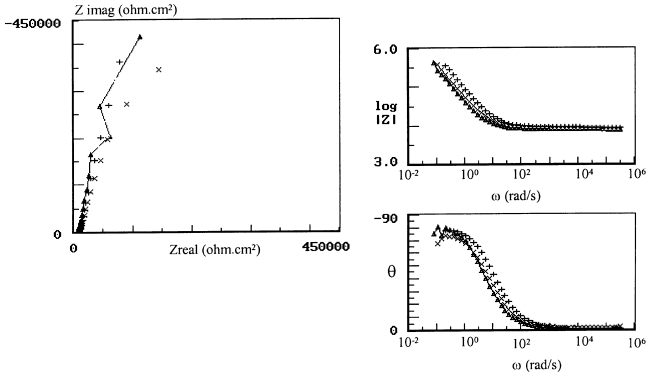

Fig. 13. Impedance spectra obtained on samples partially immersed during 7 days. (△) 0% of fly ash; (+) 15% of fly ash; (×) 30% of fly ash.

($E > -250$ mV) was observed during the first days of either total or partial immersion and is characteristic of a passive state. The state of passivity was confirmed by a capacitive response in the Bode plot and by a charge transfer resistance above 10^6 Ω cm^2.

The second range (−250, −550 mV) was observed in situations of pitting corrosion. In this condition there is

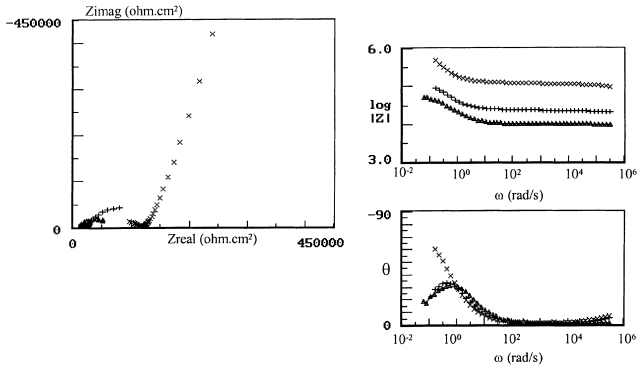

Fig. 14. Impedance spectra obtained on samples partially immersed during 180 days. (△) 0% of fly ash; (+) 15% of fly ash; (×) 30% of fly ash.

sufficient water and oxygen in the pore solution, and the passive film has been destroyed by the aggressive ions. Under these conditions, the charge transfer resistance was below 10^5 Ω cm^2. In the sample dried in air after saturation, a Warburg impedance or a transmission line developed at the low frequencies, probably consequence of the high corrosion rate and thus to limited diffusion of charged species.

The third potential range revealed values lower than −550 mV (SCE). According to ASTM C876-87 these values are characteristic of active corrosion. However, this interpretation is not totally correct, as observed in other works [13,14,16,17] and confirmed here. In fact, EIS has shown in that situation a very low corrosion rate (charge transfer resistance between 10^6 and 10^5 Ω cm^2). This is the result of insufficient oxygen supply, because the oxygen diffusivity strongly decreases in saturated concrete [5].

It is sometimes difficult to establish a boundary between the state of real activity and the state of oxygen concentration polarisation based only on potential readings. In this case, the evolution of impedance spectra can be useful in the determination of the state of

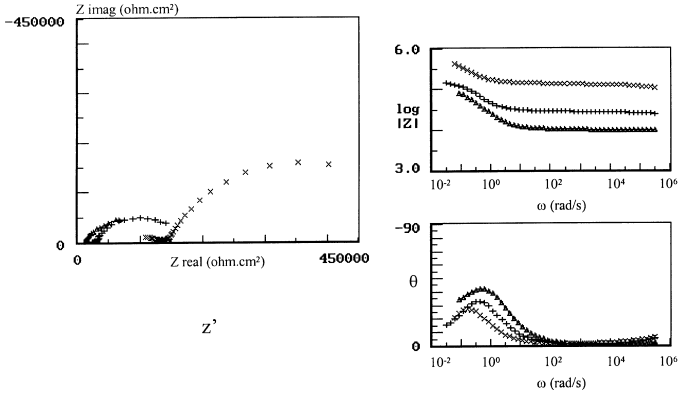

Fig. 15. Impedance spectra obtained on samples partially immersed during 540 days. (△) 0% of fly ash; (+) 15% of fly ash; (×) 30% of fly ash.

Table 3
Evolution of charge transfer resistance and OCP for samples with different fly ash contents partially immersed in 3% NaCl

Time (days)	Fly ash content (%)	R_{ct} (Ω cm^2)	E (mV) (SCE)
7	30	$>10^6$	−190
	15	$>10^6$	−156
	0	$>10^6$	−201
60	30	$>10^6$	−145
	15	1.3×10^5	−266
	0	7.6×10^4	−400
90	30	$>10^6$	−156
	15	9.6×10^4	−478
	0	7.5×10^4	−440
180	30	$>10^6$	−134
	15	8.2×10^4	−522
	0	7.4×10^4	−482
365	30	8.6×10^5	−134
	15	9.0×10^4	−522
	0	7.9×10^4	−482
540	30	4.2×10^5	−320
	15	9.2×10^4	−500
	0	7.5×10^4	−442

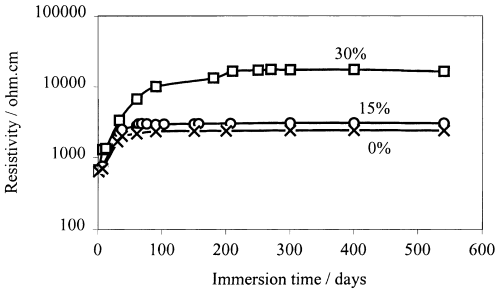

Fig. 16. Evolution of resistivity of samples partially immersed in a 3% NaCl solution.

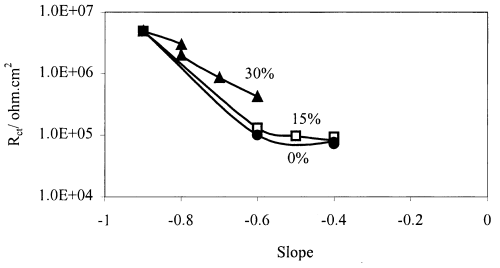

Fig. 17. Charge transfer resistance vs. the slope of the log|Z| Bode plot for the samples partially immersed in a 3% NaCl solution.

the steel surface. Impedance measurements have not just confirmed the state of corrosion/passivation, but they also allowed the determination of concrete resistivity and charge transfer resistance. The slope in the capacitive part of the spectrum decreased with the charge transfer resistance. Although this slope results from a number of factors – R_{ct}/R_s ratio, depression angle generated from surface heterogeneities or fractal surfaces [48] – the correlation was qualitatively reasonable. Another feature of the impedance spectra was the presence of a high frequency time constant. The presence of high frequency effects in impedance spectra has been observed by other authors [37,49–52], although its nature is a subject of some discussion. Some authors have attributed it to the existence of a film on the surface [28,34]. In this work the presence of this time constant seems to be related with phenomena occurring in bulk concrete. In previous work [44,45] it was shown that this time constant is also a function of the immersion time and of the fly ash content. Thus, the resistance of this time constant strongly increases with the time of immersion, following an evolution similar to that observed for the concrete resistivity. It is well defined under immersion conditions, but not in dry conditions, which also relates its nature with the bulk concrete humidity. The origin of these effects may be related with polarisation phenomena occurring in the saturated concrete pores, as suggested by other authors [52,53].

4.1. Effect of fly ash

Fly ash exerts its influence on reinforced concrete at several levels. In a study by X-ray diffraction, Koulombi et al. [54] have demonstrated that fly ash addition leads to higher chloroaluminate contents, and consequently to lower levels of free chloride, which are responsible for localised corrosion of steel. The presence of fly ash also affects the composition and thickness of the passive film. Films formed in paste solutions have revealed a thickening and a higher degree of hydration under the influence of fly ash [55].

Finally, fly ash leads to a decrease in concrete porosity, which is directly related with its resistivity. The tests on fully immersed samples have shown that for a 50% fly ash substitution, concrete resistivity was increased by a factor of 10. This result is in good agreement with the existence of an exponential law for the influence of fly ash on resistivity, as determined in previous work [44,45] and can be explained by a decrease in porosity. A lower porosity corresponds to a lower free cross-section and to an increase in path tortuosity, affecting the diffusion of solvated species. In a previous work, a reduction of chloride diffusivity in concrete to half its value was observed as a consequence of a 50% replacement of cement by fly ash [9]. The beneficial effect of fly ash concerning corrosion initiation and corrosion rate became evident in the partial immersion. In this situation samples with 30% of fly ash remained passive during about 16 months, whereas those of 0% and 15%

of fly ash became active after approximately 2 months. Also a significant reduction in corrosion rate was observed for 30% of fly ash. After 1 year of exposure the corrosion rate was lower by 1 order of magnitude when compared with the other concrete compositions. These results agree with observations from other authors, using either fly ash or slag [54,56].

The role of fly ash is thus related with both the initiation and the progression of corrosion. Fly ash is added as fine granulates and upon hydration it has the capability of partially obstructing voids and pores. This leads to a decrease of pore size and to a smaller effective diffusivity for either chloride or other species. Given the high resistance increase generated by fly ash, this effect is determinant in the long-term corrosion resistance of concrete structures.

5. Conclusions

The OCPs measured on reinforced concrete blocks fully and partially immersed in chloride-containing solution can be considered in three different ranges. The more positive range ($E > -250$ mV) revealed passivity, whereas the more negative range ($E < -550$ mV) is characteristic of oxygen diffusion limited reaction. An intermediate range ($-550 < E < -250$ mV) was observed under conditions of active iron dissolution. The boundary between the state of active corrosion and of polarisation by limited diffusion of oxygen can be difficult to establish. With this purpose, EIS has been used, revealing the state of steel surface; determination of charge transfer resistance of the corrosion reaction was made.

The use of fly ash in partial substitution of cement has lead to a higher concrete resistivity. This effect has been quantified under both complete and partial immersion. For the most aggressive conditions, i.e., partial immersion in sodium chloride solution, a 30% replacement of cement by fly ash has led to a significant increase of induction time and to a reduction of corrosion rate by 1 order of magnitude.

Acknowledgements

The first author thanks to Junta Nacional de Investigação Científica e Tecnológica (JNICT) for a Ph.D. grant. The authors gratefully acknowledge Prof. M.G.S. Ferreira for all the support provided during the project.

References

[1] Tuutti K, editor. Corrosion of steel in concrete. Swedish Cement and Concrete Research Institute, Sweden, Stockholm, 1982.
[2] Fraay ALA, Bijen JM, de Haan YM. Cement and Concrete Res 1989;19:235.
[3] Use of fly ash in concrete. ACI Commitee 226 Report, ACI Mat J, September/October 1987, p. 381.
[4] Matthews J. Concrete May/June 1992:17.
[5] Thomas MDA, Matthews J. Mater Struct 1992;25:388.
[6] Preece CM, Gronvold FO, Frolund T. In: Crane AP, editor. Corrosion of reinforcement in concrete construction. London, UK, 1983, p. 393.
[7] Lin SH. Corrosion 1990;46:964.
[8] Mangat PS, Gurusamy K. Cement and Concrete Res 1987;17:640.
[9] Salta MM. In: Swamy RN, editor. Corrosion and corrosion protection of steel in concrete. Sheffield, UK, 1994, p. 793.
[10] Montemor MF, Simões AMP, Salta MM, Ferreira MGS. Mater Sci Forum 1995;192–194:867.
[11] Montemor MF, Simões AMP, Salta MM, Ferreira MGS. In: Proceedings of the 12th International Corrosion Congress. Paper no. 76, Houston, USA (TX): NACE, 1993.
[12] Montemor MF, Simões AMP, Ferreira MGS. Corrosion 1998;54:347.
[13] Elsener B, Molina M, Bonhi H. Corros Sci 1993;35:1563.
[14] Elsener B, Bönhi H. In: Berke NS, Chaker V, Whiting D, editors. Corrosion rates of steel in concrete. ASTM STP 1065, Philadelphia, USA, 1990, p. 143.
[15] Broomfield JP, Langford PE, Ewins AJ. In: Berke NS, Chaker V, Whiting D, editors. Corrosion rates of steel in concrete. ASTM STP 1065, Philadelphia, USA, 1990, p. 157.
[16] Elsener B, Bönhi H. Mater Sci Forum 1992;111/112:635.
[17] Arup H. In: Crane AP, editor. Corrosion of reinforcement in concrete construction. London, UK, 1983, p. 151.
[18] Browne RD, Geoghegan MP, Baker AF. In: Crane AP, editor. Corrosion of reinforcement in concrete construction. London, UK, 1983, p. 193.
[19] Gonzalez JA, Algaba S, Andrade C. Br Corros J 1980;15:135.
[20] Gonzalez JA, Andrade C. Br Corros J 1982;17:21.
[21] Carassiti F, Proverbio E, Valente T. Mater Sci Forum 1992;111/112:647.
[22] Macdonald DD, Urquidi-Macdonald M, Filho RC, El-Tantawy Y. Corrosion 1991;47:330.
[23] Feliu S, Gonzalez JA, Escudero ML, Andrade C. Corrosion 1990;46:1015.
[24] Gonzalez JA, Benito M, Feliu S, Rodríguez P, Andrade C. Corrosion 1995;51:145.
[25] Moosavi AN, John DG, Gedge G. In: Swamy RN, editor. Corrosion and corrosion protection of steel in concrete. Sheffield, UK, 1994, p. 116.
[26] Broomfield JP. In: Swamy RN, editor. Corrosion and corrosion protection of steel in concrete. Sheffield, UK, 1994, p. 1.
[27] Rodriguez J, Ortega LM, Garcia AM. In: Swamy RN, editor. Corrosion and corrosion protection of steel in concrete. Sheffield, UK, 1994, p. 171.
[28] John DG, Searson PC, Dawson JL. Br Corros J 1981;16:102.
[29] Noggerath J, Böhni H. Mater Sci Forum 1992;111/112:659.
[30] Keddam M, Nóvoa XR, Soler I, Andrade C, Takenouti H. Corros Sci 1994;36:1155.
[31] Triki E, Dhouibi-Hachani L, Raharinaivo A. In: Proceedings of the 12th International Corrosion Congress, Houston, TX, USA, 1993.
[32] Newton CJ, Sykes JM. Corros Sci 1988;11:1051.
[33] Feliu S, Gonzalez JA, Andrade C, Feliu V. Corros Sci 1986;26:961.
[34] Lay P, Lawrence PF, Wilkins NJM. J Appl Electrochem 1985;17:755.
[35] Lemoine L, Wenger F, Galland J. In: Berke NS, Chaker V, Whiting D, editors. Corrosion rates of steel in concrete. ASTM STP 1065, Philadelphia, USA, 1990, p. 118.

[36] Glass GK, Asseinein AM, Buenfeld NR. Corrosion 1988;54:887.
[37] Feliu V, Gonzalez JA, Andrade C, Feliu S. Corros Sci 1988;40:975.
[38] Feliu V, Gonzalez JA, Andrade C, Feliu S. Corros Sci 1988;40:995.
[39] Mansfeld F. Corrosion 1988;44:857.
[40] Oltra R, Keddam M. Corros Sci 1988;28:1.
[41] Mansfeld F, Kending MW, Tsai S. Corrosion 1982;38:478.
[42] Pourbaix M. In: Gauthier-Villars C, editor. Atlas d'equilibres electrochimiques, Paris, France, 1963.
[43] Searson PC. Ph.D. Thesis, Manchester, UK, 1982.
[44] Montemor MF, Simões AMP, Salta MM, Ferreira MGS. Corros Sci 1993;35:1571.
[45] Montemor MF, Simões AMP, Salta MM, Ferreira MGS. In: Swamy RN, editor. Corrosion and corrosion protection of steel in concrete. Sheffield, UK, 1994, p. 751.
[46] Andrade C, Soler L, Alonso C, Nóvoa XR, Keddam M. Corros Sci 1995;37:2013.
[47] Sehgal A, Kho YT, Osseo-Asare K, Pickering HW. Corrosion 1992;48:871.
[48] Geenen F. Ph.D. Thesis. The Netherlands: T.U. Delft, 1991.
[49] Noggerath J, Bönhi H. Mater Sci Forum 1986;44/45:856.
[50] Dawson JL, In: Crane AP, editor. Corrosion of reinforcement in concrete construction. London, UK, 1983, p. 175.
[51] Wenger F, Galland J. Mater Sci Forum 1983;44:375.
[52] Carter WJ, Garvin S. J Phys D 1984;22:1773.
[53] Keddam M, Takenouti H, Nóvoa XR, Andrade C, Alonso C. In: Study of the dielectric characterisation of cement paste, EM-CRVI: Trento, Italy, 1997, Published in: Mater Sci Forum, Trans Tech Publications, 1988;289–292:15.
[54] Koulombi N, Batis G, Malami CH. In: Costa JM, Mercer AD, editors. Progress in the understanding and prevention of corrosion, vol. 1. The Institute of Materials, Spain, 1993, p. 619.
[55] Montemor MF, Simões AMP, Ferreira MGS. Corrosion 1998;54:347.
[56] Dehghanian C. Corrosion 1999;55:291.